Enhancing the demulsification performance using metal-organic frameworks with amphipathic microdomain

Rui Wang[1], Yi Feng[1], Haijun Xu[1], Huijun Cai[1], and Ying Zhou[1]

[1]Affiliation not available

May 5, 2020

Abstract

Demulsification is an important process for dehydration of crude oil and environmental remediation. The intrinsic structure of metal-organic frameworks (MOFs) endows MOFs with amphipathicity and meets the requirement of demulsifier. Herein, we studied the demulsification performance, process and characteristic using MIL-100(Fe). The amphipathicity of MIL-100(Fe) is crucial for demulsification. The demulsification efficiency (DE) for model emulsion excessed 99% within 30 min at optimal condition, and dehydration efficiency for crude oil emulsion was up to 79% within 5 min. The DE can be maintained when the pH ranged from 10.0 to 4.0, and it increased along with an increase of salinity (1~1000 mmol*L-1). Component analysis revealed that the degradation of sodium dodecyl sulfonate occurred by an abstraction of SO32-, which could eliminate the potential risk of emulsifying again. Therefore, this study confirmed that enhancing the interaction with emulsion is an effective strategy for new demulsifier to against the harsh conditions.

Enhancing the demulsification performance using metal-organic frameworks with amphipathic microdomain

Rui Wang[1,2], Yi Feng[1], Haijuan Xu[3], Huijun Cai[1] and Ying Zhou[1,2,*]

(1. State Key Laboratory of Oil and Gas Reservoir Geology and Exploitation, Southwest Petroleum University, Chengdu 610500*, China)*

(2. The Center of New Energy Materials and Technology, School of New Energy and Materials, Southwest Petroleum University, Chengdu 610500*, China)*

(3. Department of Chemistry and Environmental Engineering, Hubei Minzu University, Enshi 445000*. China)*

[*]Corresponding author: Ying Zhou; Fax: +86 28 83037406; E-mail:*yzhou@swpu.edu.cn*; Postal address: School of New Energy and Materials, Southwest Petroleum University, No. 8, Xindu Road, Chengdu 610500, China.

Abstract: Demulsification is an important process for dehydration of crude oil and environmental remediation. The intrinsic structure of metal-organic frameworks (MOFs) endows MOFs with amphipathicity and meets the requirement of demulsifier. Herein, we studied the demulsification performance, process and characteristic using MIL-100(Fe), a kind of classical MOFs. It was found that the amphipathicity of MIL-100(Fe) is crucial for demulsification. The demulsification efficiency (DE) for model emulsion excessed 99% within 30 min at optimal condition, and dehydration efficiency for crude oil emulsion was up to 79% within 5 min using MIL-100(Fe). The DE can be maintained when the pH ranged from 10.0 to 4.0, and it increased along with an increase of salinity (1~1000 mmol·L^{-1}). Component analysis revealed that the degradation of sodium dodecyl sulfonate occurred by an abstraction of SO_3^{2-}, which could eliminate the potential risk of emulsifying again. Therefore, this study exhibited the potential of MIL-100(Fe) for demulsification, and

confirmed that enhancing the interaction with emulsion is an effective strategy for new demulsifier to against the harsh conditions.

Key words: Demulsification, MOFs, amphipathic microdomain, harsh conditions, degradation

Topical area : Energy and environmental engineering

1. Introduction

As consumption of energy, conventional oil resource decreases sharply[1-2]. In order to enhance the yield of oil, the most common method is injecting water into the oil well [3]. Although this strategy can improve the output of crude oil, it meanwhile caused high water content for crude oil and pollution for environment[3~5]. The crude oil with high water content generally exists with stable emulsion [5,6], which can corrode pipeline and refining equipment [3,5]. Moreover, emulsion can form from the wastewater containing oil with the help of surfactant in water, which could scatter the sunlight, hamper the input of energy for aquatic system and increase the (bio-) chemical oxygen demand (COD/BOD)[4,7]. All above will cause local aquatic system anoxic, and reduce the water quality. Emulsion also raises the migratory risk of toxic and insoluble pollutants, and enlarges the difficulty of remediation for pollution[4,7,8]. As a result, the remove of both oil and emulsion in water is important for the environmental remediation. Compared with the oil/water separation [9,10], the removalof emulsion is a challenge because of its high stability. Therefore, the demulsification has become one of the focuses for the petroleum industry and environment.

Compared with physical and biological methods, the chemical demulsification is effective, energy-saving and fast[11-13]. An ideal demulsifier has the characteristics of large surface area ($nm^2 \cdot molecule^{-1}$) and amphipathicity [6,14]. The mechanism of demulsification for conventional demulsifier is competing with surfactant on the interfacial film to decrease the interface tension (IFT) and accelerate the coalescence of emulsion [6,13,15]. The driving force of demulsification for the conventional demulsifier is supramolecular interaction[15], which is weak and make demulsification performance influenced frequently by the practical conditions, such as salinity, pH and so on [6,9,16]. Typically, counter ions can shrink the double electric layer along with an increase of hydration for the interface of emulsion, enhancing the stability of emulsion and decreasing demulsification efficiency of conventional demulsifier[17]. Additionally, the conventional demulsifier need relatively long time to obtain satisfying performance[18-20]. Furthermore, the weak supramolecular interaction limits the improvement of demulsification performance. Thus, enhancing the interaction between demulsifier and emulsion could be a potential strategy to conquer the shortcomings of those conventional demulsifiers.

Most of conventional demulsifiers are soluble, such as ethylene oxide/propylene oxide (EO/PO) segmented copolymer, dendritic polymer with amine group, polyether and ionic liquid [17,21]. The soluble demulsifier is also a potential pollutant, which increases the cost and burden of environment. Recently, heterogeneous demulsifier has attracted much attention due to the merit of recyclability and environment-friendly [22-24]. Metal-organic frameworks (MOFs) are functional crystal materials, which are consisted of polar node and non-polar bridge. This structure ensures a special microdomain with amphipathicity [25], meeting the design of molecular structure of demulsifier. The node of MOFs is strong Lewis acid or Brønsted acid site [26,27], which can react with the species contained oxygen (O), nitrogen (N), sulfur (S) and so on by coordination, ligand/ion exchange and electrostatic interaction[28,29]. It should be noted that the surfactant covered on emulsion consists of hydrophobic alkyl chain and hydrophilic group, which usually contained O, N or S. And the crude oil also contained heteroatomic (O, S and N) at some degree [30]. Therefore, there is potential strong interaction between the node of MOFs and emulsion. Meanwhile the non-polar bridge of MOFs can interact with organic species by the supramolecular interaction, which could promote the coalescence of oil phase when the polar node of MOFs interacts with emulsion. What's more, the pore of MOFs can regulate the existing states of surfactant or oil phase molecule. All of these properties of MOFs could bring some different features for the demulsification, compared with that of the conventional demulsifier. To the best of our knowledge, the MOFs do not gain due attention as an intrinsic heterogeneous demulsifier.

Herein, we prepared the MIL-100(Fe), a classical MOFs, as an intrinsic heterogeneous demulsifier. Then, the demulsification performances both for model emulsion and crude oil emulsion were investigated by batch

experiments using MIL-100(Fe). The process of demulsification was studied by the inverted microscope. Moreover, the interactional characteristics between the MIL-100(Fe) and model emulsion were revealed by the surface measurement and component analysis.

2. Experiments

2.1 Chemicals

Ferric chloride hexahydrate ($FeCl_3 \cdot 6H_2O$), trimesic acid (BTC), methanol, sodium dodecyl sulfate (SDS), oleic acid, petroleum ether were analytic reagents without purification further. The crude oil with a density of 0.77 $g \cdot cm^3$and a viscosity of 13.9 $mN \cdot s \cdot m^{-1}$ at 20 was obtained from an oilfield at Tarim Basin, China.

2.2 Preparation of material

The material was prepared with a modified method from literatures [31,32]. Typically, 200 mL of methanol solution contained 10.50 g of BTC was dropped into 250 ml of $FeCl_3$ solution (0.3 $mol*L^{-1}$) at a condition of stirring vigorously. The saffron sediment was washed several times with ultrapure water (18.25 $M\Omega \cdot cm^{-1}$) and ethanol following stirring 12 h at room temperature. Then, the saffron product was dried at 60 in oven.

2.3 Characterization

The as-prepared material was characterized by X-ray diffraction (XRD, PANalytical) and scanning electron microscope (SEM, FEI Quanta430 microscope) to identify the structure and morphology. The pore structure was measured by N_2 isothermal adsorption/desorption. The distribution of size and wettability for the as-prepared material were measured by dynamiclightscattering (DLS) (Marlven Nano-ZS, England) and video contact angle analyzer (Dataphysics OCA25, German). The parameters for XRD measurement and the methods for the analysis of pore structure were shown in the supporting information (**Text S1**).

2.4 Demulsification study

Firstly, 40 ml of oleic acid was added into 200 ml of ultrapure water contained 0.2 g of SDS, stirring by the homogenizer at a speed of 3800 $rpm*min^{-1}$, to prepare the model emulsion. The model emulsion was used after diluting by ultrapure water in the next investigation. The concentration of model emulsion was expressed with a volume ratio ($v*v^{-1}$) of oleic acid in water.

Initially, demulsification performance was investigated at different conditions of dosage, concentration, time, pH and salinity using the as-prepared material. The regenerability was studied following washing used material with ethanol and petroleum ether. Typically, 0.10 g of the as-prepared material was suspended in 19.6 ml ultrapure water, then 0.4 ml of the model emulsion was added into the as-prepared material suspension. After that, the suspension contained as-prepared material and model emulsion was silence following shock drastic. And the cycle of shock-silence did several times in 30 min. Subsequently, the suspension was filtrated. The filter liquor was extracted by petroleum ether. The absorbance of extracted liquor was measured at 268 nm by a UV-vis spectrophotometer (Shimadzu, UV-2600). The demulsification efficiency (DE) was calculated according to the **Eq. 1** :

$DE = (A_0 - A_1)/A_0 \times 100\%$ (**Eq. 1**)

Where, DE (%) was the demulsification efficiency for the model emulsion using the as-prepared material, A_0 and A_1 were absorbances of extract liquors before and after demulsification.

To exhibit the demulsification process, the demulsification phenomenon was recorded by an inverted microscope (AMG EVOSFL, Amercian). The interaction between as-prepared material and model emulsion was reveal by attenuated total reflection infrared spectroscopy (ATR-IR, Nicolet iS5,Thermo Fisher Scientific), X-ray photoelectron spectroscopy (XPS, ES CALAB 250Xi, Thermo Fisher Scientific) and Zeta potential (Marlven Nano-ZS, England). Additionally, the components of SDS solution after interacting with as-prepared material were measured by ion chromatogram (IC) and liquid chromatogram-mass spectroscopy (LC-MS).

3. Results and discussion

3.1 Structure and morphology

The XRD pattern of as-prepared material was presented in **Fig. 1a** . It showed the characteristic peaks at a range of 5deg ~ 30deg, which were in good agreement with that of MIL-100(Fe) [32], indicating that the MIL-100(Fe) was successfully synthesized by this method. The size of as-prepared MIL-100(Fe) was c.a. 300 nm (**Fig. 1b**), which agreed with an average diameter of 242(+-52) nm measured by DLS (Fig. S1). In addition, the specific surface area, total pore volume and porosity of as-prepared MIL-100(Fe) were 1344 m^2*g^{-1}, 0.727 cm^3*g^{-1} and 89.7%, respectively (**Fig. S2** and **Table S1**).

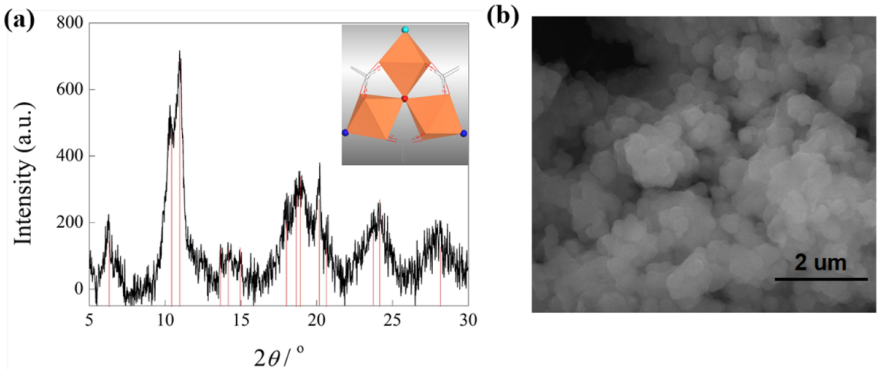

Fig. 1 XRD pattern (**a** , the insert was structure unit of MIL-100(Fe)) and SEM image of as-prepared MIL-100(Fe) (**b**)

3.2 Demulsification performances

Amphipathicity was a crucial characteristic for demulsifier[6,14]. Therefore, the wettability of the obtained MIL-100(Fe) was measured initially. As showed in Fig. S3, the water and oleic acid drops permeated into the plane of MIL-100(Fe) quickly, which suggested that the MIL-100(Fe) was amphipathic. Subsequently, the demulsification performance was investigated using MIL-100(Fe) as a heterogeneous demulsifier. Compared with the homogeneous milky model emulsion (an average diameter of 2.53 um), the demulsified liquid was transparent without obvious emulsion drops (**Fig. 2a** and **2b**). The demulsified MIL-100(Fe) floated on the water (**Fig. 2a**), which confirmed that the oil phase released from emulsion drops by the MIL-100(Fe). At an optimal condition of dosage and concentration, the DE can exceed 99% (**Fig. S4**).

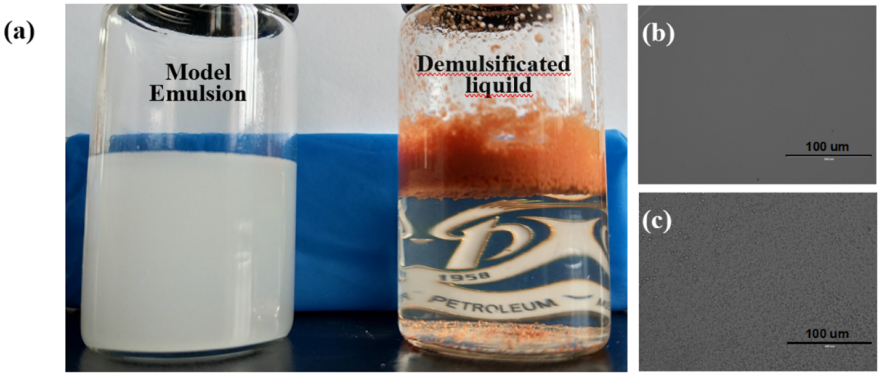

Fig. 2 Photographs of the demulsification phenomenon (**a**) (the dosage of MIL-100(Fe) and concentration of model emulsion were 1% ($w \cdot w^{-1}$) and 1:250 ($v \cdot v^{-1}$)), microscope photographs of the demulsified liquid (**b**) and model emulsion (**c**)

To investigate the influence of time, pH and salinity on the demulsification performance of MIL-100(Fe), the rest demulsification was carried out with a 0.5% ($w \cdot w^{-1}$) of MIL-100(Fe) and 1:250 ($v \cdot v^{-1}$) of model emulsion. As showed in**Fig. 3a** , the DE exceeded 86% of maximum demulsification capacity within 1 min, and the saturated demulsification time was no more than 30 min. When the pH was 2.0, the DE was 97%. As increasing for pH from 4.0 to 10.0, the DE maintained around 90% (**Fig. 3b**). Besides, the DE increased from 92% to 98%, following a rise of the salinity (1 $mmol \cdot L^{-1}$ ~ 1000 $mmol \cdot L^{-1}$) (**Fig. 3c**). What's more, a DE of 95% indicated that the demulsification performance of MIL-100(Fe) was not inhibited by the 10 $mmol \cdot L^{-1}$ of Mg^{2+} solution. Generally, the concentrated electrolyte could weaken the electrostatic attraction by shrinking the double electric layer and supramolecular interaction by increasing the hydration, thus decreasing the demulsification performance of demulsifier [17]. But this was contrary to the results in this work, which implied that the interaction between MIL-100(Fe) and emulsion was more powerful than that of the conventional demulsifiers. Afterwards, the regenerability of MIL-100(Fe) was studied. The DE of the used MIL-100(Fe) decreased by 14% and 36% after 2th and 3th cycles (**Fig. 3d**). The reason of decrease for the demulsification performance might be related to the change of wettability for the used MIL-100(Fe), which was illuminated by the following study.

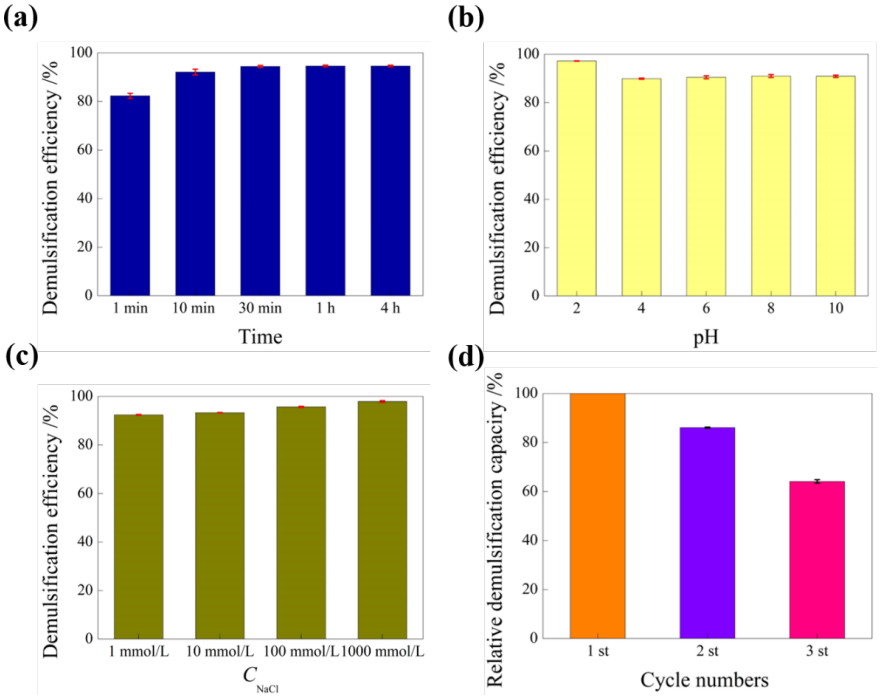

Fig. 3 Demulsification efficiencies of MIL-100(Fe) at different time (**a**), pH (**b**) and salinity (**c**), and that of the used MIL-100(Fe) (**d**)

Above investigation for demulsification performance suggested that MIL-100(Fe) can demulsify perfectly, especially at the acid and hyperhaline environment, which exactly was the conditions of exploiting for the oil [33,34]. Therefore, the MIL-100(Fe) is suitable for demulsification in the area of the petroleum industry.

Furthermore, the dehydration for crude oil emulsion was carried out to investigate the practical demulsification performance of MIL-100(Fe). Shocking drastically about 10 s following adding 0.50 g of MIL-100(Fe)

into 50 ml of crude oil emulsion with a water content of 90%, the crude oil and water separated spontaneously within 5 min at room temperature without any other assistive technologies (**Fig. S5**). The dehydration efficiency for crude oil emulsion using MIL-100(Fe) was 79%. Particularly, the time for the dehydration of crude oil emulsion was very short, compared with the conventional demulsifier (˜hour) [35-37]and some loading type heterogeneous demulsifier (exceed 30 min)[38,39]. It should be noted that the dehydration efficiency for crude oil emulsion using MIL-100(Fe) might be further improved through the optimization of dehydration conditions and the combination with other assistive technologies.

3.3 Demulsification process

To investigate the demulsification process, the demulsification was recorded by an inverted microscope. As presented in **Fig. 4a** , a lot of floccules formed as soon as contacting with the emulsion. And the rounded edge of emulsion drop was replaced by the irregular margin of large floccules. The coalescence for emulsions could occur with different patterns, such as two points coalescence liking the cell fusion (**Fig. 4b**), three points blend (**Fig. 4c**) and multi-point incorporation (**Fig. 4d**). Finally, the coalesced emulsion drops would crack as shown in the **Fig. 4e** , releasing the oleic acid. The oleic acid surrounded the MIL-100(Fe), forming the floccules and floating on the water as showed in **Fig. 2a** .

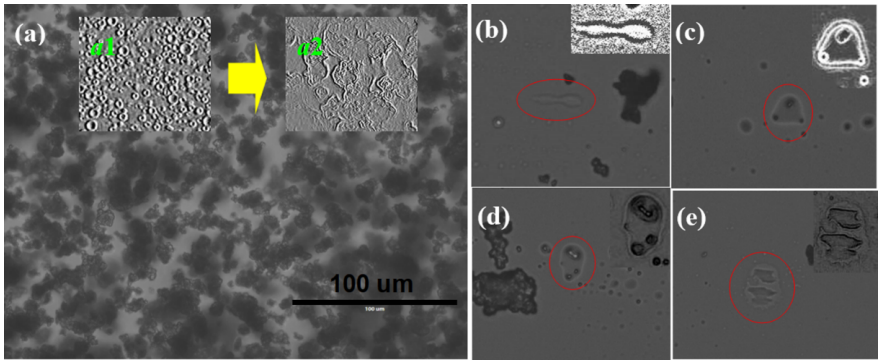

Fig. 4 Photographs for the demulsification process (**a** was the image of demulsification, the insert of$a$**1** and a**2** were the embossment of edge before and after demulsification.**b** ˜**d** were the representative coalescence modes of emulsion, and **e** exhibited the moment of cracking for the coalesced emulsion drop)

The fast fusion for emulsion drops during the demulsification process can be explained by the amphipathicity of MIL-100(Fe). The hydrophilic domain of MIL-100(Fe) ensured the contact with the interface film of emulsion, so that it was beneficial for MIL-100(Fe) to adhere on the emulsion drops. Meanwhile, the lipophilicity domain of MIL-100(Fe) can enhance the fusion of emulsion drops by the hydrophobic interaction, which was supported by the facts that the oleic acid drop permeated into the waterwetted MIL-100(Fe) quickly (**Fig. S6**).

The model for oleic acid permeates horizontally on the water wetted MIL-100(Fe) was presented in **Fig. 5** . The$f_{\mathrm{Attraction}}$, which stands for apparent affinity of oleic acid on the waterwetted MIL-100(Fe), can be expressed as the**Eq. 2** . In this study, the oleic acid is newton liquid, which has a constant viscosity at a certain temperature. That is the inner resistance to oleic acid ($f_{\mathrm{Viscosity}}$) against motion is constant and equal to the viscosity. The outer resistance against motion for the permeation is from hydrophobicity ($f_{\mathrm{Hydrophobicity}}$) because of the layer of hydration covered on MIL-100(Fe). It was difficult to record permeation in situ. Herein, we instead the accelerated speed of$a$ (**Eq. 3**) with average accelerated speed of$\overline{a}$ (**Eq. 4**) along with a change of$F_{\mathrm{Attraction}}$ by$\overline{F}_{\mathrm{Attraction}}$ (average apparent affinity). Giving a hypothesis of unit volume V for oleic acid, there are $m = 0.89V$, where 0.89 (kg·m^{-3}) is the density of oleic acid at 20 . Then, the$\overline{F}_{\mathrm{Attraction}}$ is$(1.78V\frac{L}{t^2} + 35.3 \times 10^{-3}\ \mathrm{N} + f_{\mathrm{Hydrophobicity}})$, where the items of $1.78V\frac{L}{t^2}$ and$f_{\mathrm{Hydrophobicity}}$ are positive. Therefore, the$\overline{F}_{\mathrm{Attraction}}$ is more than the surface tension of oleic acid (33.8×10^{-3} N). This

indicated the oleic acid can access to the MIL-100(Fe) without inhibiting of hydration even in water, which caused the fast fusion of emulsion drops as shown in **Fig. 4** . This conclusion is in good agreement with the stable demulsification performance against the pH and salinity (**Fig. 3b** and **Fig. 3c**).

$F_{\text{Attraction}} - f_{\text{Viscosity}} - f_{\text{Hydrophobicity}} = m \cdot a$**Eq. (2)**

$a = \nabla^2 \frac{\partial L}{\partial t}$**Eq. (3)**

$\overline{a} = \frac{2L}{t^2}$**Eq. (4)**

Where, the $F_{\text{Attraction}}$ is the apparent affinity for oleic acid on thewater wetted MIL-100(Fe), m is the mass of oleic acid, $f_{\text{Viscosity}}$ is the resistance because of viscosity (the viscosity of oleic acid is $35.3\text{x}10^{-3}\text{N*s*m}^{-1}$ at 20[40]),$f_{\text{Hydrophobicity}}$is the force originated from hydrophobicity, a is the accelerated speed of motion for permeation, L is the distance for permeation,t is the time for permeation, $\overline{a}$ is the average accelerated speed of motion for permeation.

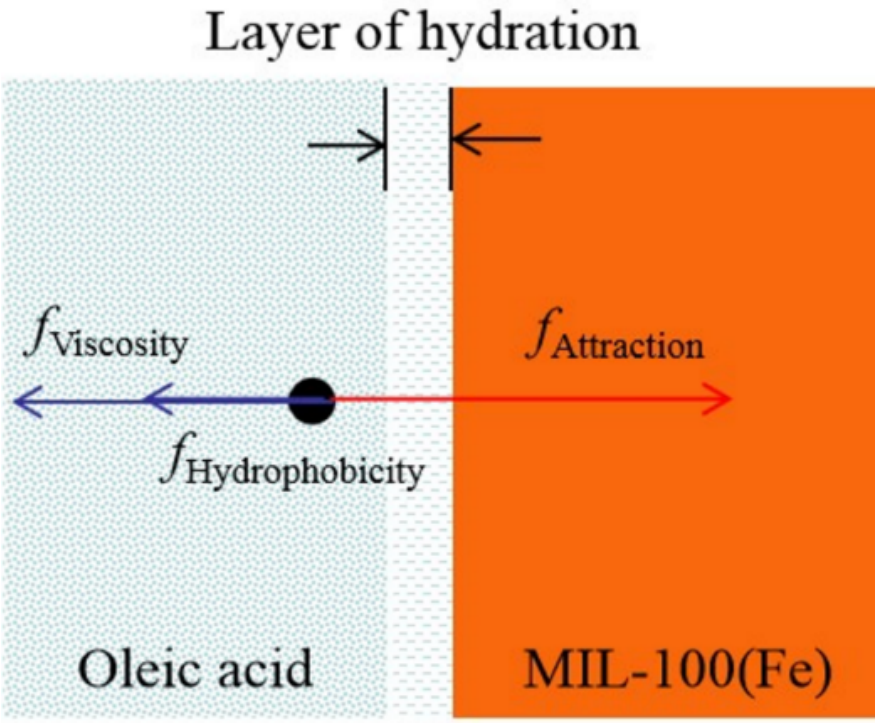

Fig. 5 Model for oleic acid permeates horizontally on the water wetted MIL-100(Fe)

Furthermore, the wettability of used MIL-100(Fe) was studied. With pressing continuously, the water drop was deformative and rolled on the plane of used MIL-100(Fe) (**Fig. 6a˜e**). Additionally, the static water contact angle (WCA) of used MIL-100(Fe) was up to 179° (**Fig. 6f**). Those characteristics of used MIL-100(Fe) suggested that the wettability of used MIL-100(Fe) has changed from amphipathicity to hydrophobicity, and the force of adhere for water on the used MIL-100(Fe) was extremely weak. The hydrophobicity was disadvantage for the contact between the used MIL-100(Fe) and emulsion drops. Therefore, the demulsification performance of used MIL-100(Fe) decreased dramatically (**Fig. 3d**).

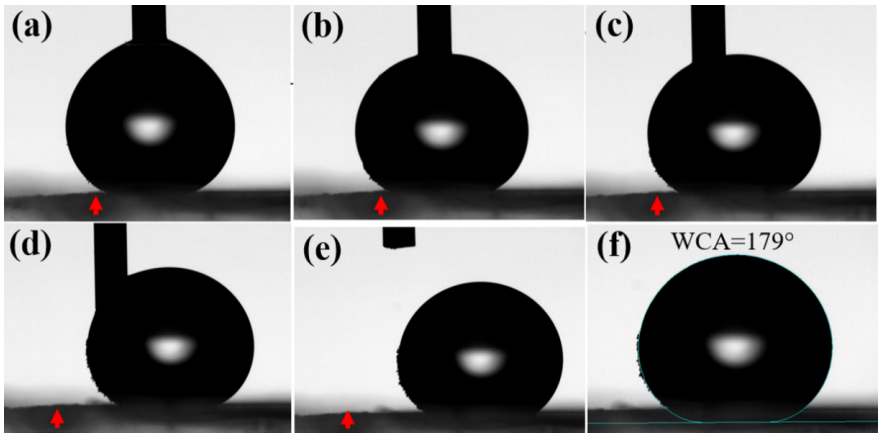

Fig. 6 Wettability for a water drop on the plane of used MIL-100(Fe) (**a˜e** shown the dynamic behaviors of a water drop with a continuous pression, the red arrow was the location for reference) (**f** shown the static water contact angle)

3.4 Interaction for demulsification

As mentioned above, the hydrophilic domain of MIL-100(Fe) was the key point of demulsification. However, the interaction between the hydrophilic domain of the MIL-100(Fe) and emulsion was not understood well. In order to uncover the interaction, the fresh and used MIL-100(Fe) were measured by ATR-IR and XPS. Compared with the fresh MIL-100(Fe), the symmetric vibration absorption band of carboxylate ($\nu_{as(COO)-}$) for the used MIL-100(Fe) changed unsymmetrically and was blue shift (**Fig. 7a**). While the vibration absorption band of FeO_6 octahedron for the used MIL-100(Fe) at 619 cm^{-1} was red shift[32] (**Fig. 7b**). What's more, the new absorption band of alkyl chain (-CH_2-) at 2855 cm^{-1} and 2927 cm^{-1}**(Fig. 7c**) suggested the organic species were remained in the MIL-100(Fe) after demulsification. The residual alkyl chain could decrease the surface energy of used MIL-100(Fe), causing a hydrophobic surface. The XPS results of the used MIL-100(Fe) presented in **Fig. 7d** displayed that a signal of Fe^{2+} appeared at 709.1 eV, and the relative content for the unsaturated $Fe^{3+}$to the saturated Fe^{3+} changed from 45% to 95%[28]. The change for the Fe^{3+}implied the reaction between the node of MIL-100(Fe) and the model emulsion might exist. However, what most interesting was that there was no signal of S in the XPS for the used MIL-100(Fe) (**Fig. S7**).

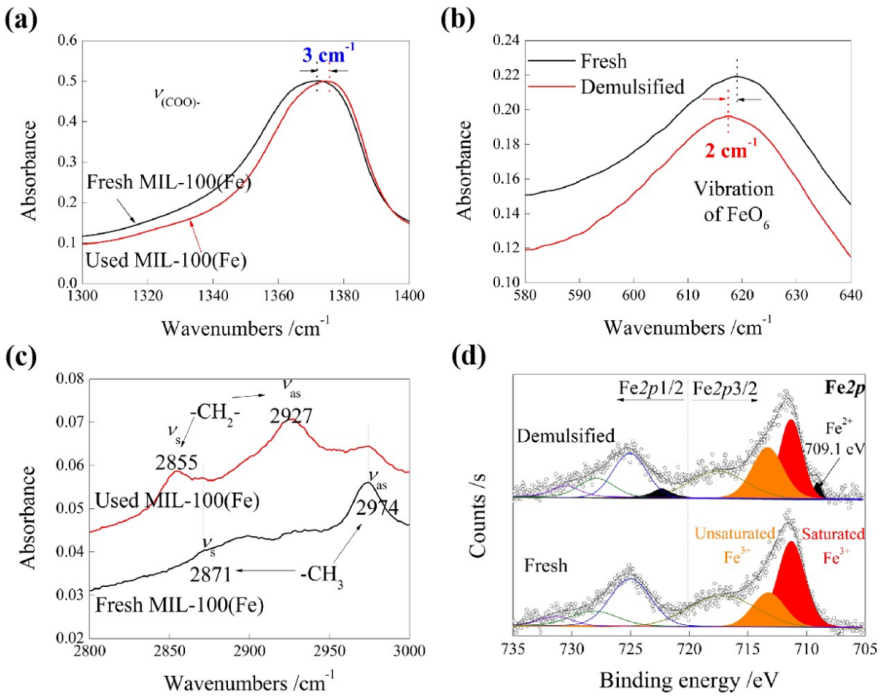

Fig. 7 ATR-IR and XPS for the fresh and used MIL-100(Fe) (**a** ~**c** were the results of ATR-IR, **d** was the result of XPS)

In order to make it clear what happened for the SDS covered on the model emulsion. The component of the SDS solution after interaction with MIL-100(Fe) was detected by ion chromatogram (IC) and liquid chromatogram-mass spectroscopy (LC-MS). The result of IC suggested that the SO_3^{2-} or SO_4^{2-} was released from SDS after interaction with MIL-100(Fe) (**Fig. 8**). What's more, MIL-100(Fe) degraded the SDS obviously according to the results of LC-MS (**Fig. S8**). The hydrogenation peak at m/z =187 verified that the degradation products contained dodecyl alcohol ($CH_3(CH_2)_{10}CH_2OH$, M=186) (**Fig. S9**), which implied that the group of SO_3^{2-} instead of SO_4^{2-}, was prefer to be extracted from SDS when the MIL-100(Fe) interacted with SDS. The dodecyl alcohol could be oxidized into undecyl carboxylic acid ($CH_3(CH_2)_{10}COOH$, M=200) with a molecule ion peak at m/z =199 (**Fig. S9**) further. After interaction with SDS, the BTC with a molecule ion peak atm/z =209 (**Fig. S10**) was released from MIL-100(Fe). The components with retention time of 4.6 min (m/z =223) and 5.1 min (m/z =237) were the ester and binary ester of BTC with formulas of $C_8H_5O_6CH_3$and $C_8H_4O_6(CH_3)_2$(**Fig. S11** and **Fig. S12**). Those esters might be the residues when the MIL-100(Fe) was prepared, because there were absorption band of C-H for CH_3 at 2871 cm^{-1} and 2974 cm^{-1} and absorption band of C-O-C for esters at 1088 cm^{-1} in the ATR-IR results of fresh MIL-100(Fe) (**Fig. S13**). The leaching for BTC, $C_8H_5O_6CH_3$and $C_8H_4O_6(CH_3)_2$implied that the structure of MIL-100(Fe) was destroyed at some degree, which can cause the changes of absorbance for the carboxylate and -CH_3 group as showed in **Fig. 7a** and**7c** .

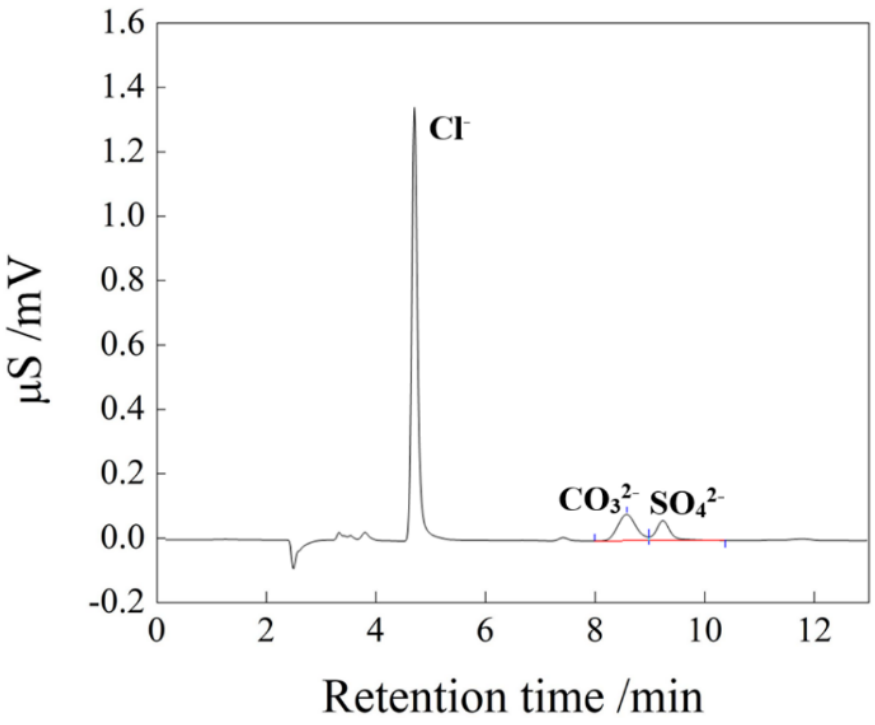

Fig. 8 Ion chromatogram (IC) of SDS solution after interaction with MIL-100(Fe)

Above IC and LC-MS results confirmed that the SDS was degraded by MIL-100(Fe). However, this reaction with SDS did not influence the crystal structure of MIL-100(Fe) obviously, because XRD pattern of the used MIL-100(Fe) was the same as that of the fresh MIL-100(Fe) (**Fig. S14**).

Finally, the influence of electrostatic interaction on the demulsification was studied by the zeta potentials and demulsification efficiencies for different model emulsions. The negative charge increased continuously because of hydroxylation [41]when the pH was increased from 4.0 to 10.0 (**Fig. 9a**). The zeta potentials of MIL-100(Fe) and model emulsion at the condition of demulsification were 19.8 mV and -67.2 mV, which suggested that there was electrostatic attraction between MIL-100(Fe) and model emulsion stabilized by SDS. And the electrostatic attraction weakened along with an increased of pH, which would decrease the adsorption capacity droved by the electrostatic attraction for emulsion on MIL-100(Fe). Therefore, the DE would decrease when the pH increased. But the results of demulsification performance shown that the DE of MIL-100(Fe) maintained around 90% with the range of pH (4˜10) (**Fig. 3b**). Additionally, the DE for the model emulsion stabilized by Tween 80, a kind of nonionic surfactant, was up to 91% using MIL-100(Fe) at the same conditions (**Fig. 9b**). It could conclude that the contribution of adsorption droved by the electrostatic attraction on demulsification was minor. However, the electrostatic repulsion hampered contact with MIL-100(Fe) and emulsion, causing a low demulsification efficiency for the model emulsion stabilized by cetyl ammonium bromide (CTAB, a kind of cationic surfactant) (**Fig. 9b**).

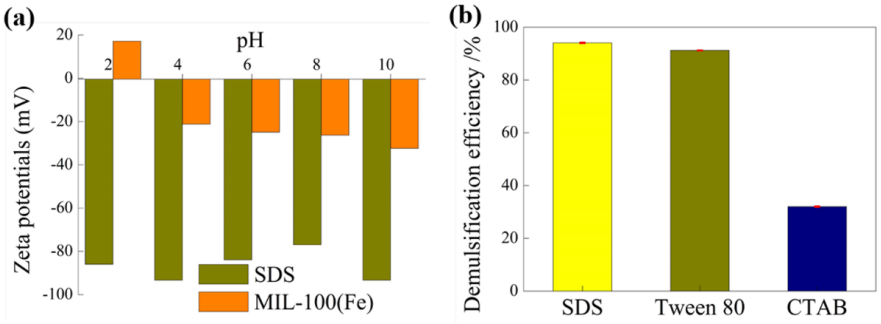

Fig.9 Zeta potentials of MIL-100(Fe) and model emulsion stabilized by SDS at different pH ((**a**), the concentrations of MIL-100(Fe) and emulsions were 0.1 g·L^{-1} and 1:250), demulsification efficiencies for model emulsions stabilized by different surfactants (**b**)

4. Conclusion

In summary, MIL-100(Fe) exhibited excellent demulsification performance for the model emulsion. The MIL-100(Fe) preferred to demulsify at acid and hyperhaline conditions. The amphipathicity micro-domain of MIL-100(Fe) was important for demulsification. MIL-100(Fe) degraded the SDS by abstracting the hydrophilic group of SDS. This degradation for surfactant could erase the potential risk of emulsifying again. At the practical occasion, MIL-100(Fe) dehydrated the water of 79% from the crude emulsion within 5 min without any without any other assistive technologies. Therefore, this study exhibited the potential of demulsification using MOFs in the area of environmental remediation and petroleum industry. Additionally, this study could be a guidance for the development of new demulsifier to against the harsh conditions.

Acknowledgements

This work was supported by National Natural Science Foundation of China [U1862111] and Graduate Scientific Research Innovation Foundation of SWPU [2019cxzd012].

Interests statement

This paper has not any interests conflict with other person and organization.

Appendix A. Supplementary data

Supplementary data associated with this article can be found, in the online version.

Reference

[1] American Association of Petroleum Geologists, Energy Minerals Division. Unconventional energy resources: 2017 review. Natural Resources Research. 2019;28:1661–1751.

[2] Mohr SH, Wang J, Ellem G, Ward J, Giurco D. Projection of world fossil fuels by country. Fuel. 2015;141:120–135.

[3] Epelle EI, Gerogiorgis DI. Optimal rate allocation for production and injection wells in an oil and gas field for enhanced profitability. AICHE Journal. 2019;65:16592.

[4] Putatunda S, Bhattacharya S, Sen D, Bhattacharjee C. A review on the application of different treatment processes for emulsified oily wastewater. International Journal of Environmental Science and Technology. 2019;16:2525–2536.

[5] Saad MA, Kamil M, Abdurahman NH, Yunus RM, Awad OI. An overview of recent advances in state-of-the-art techniques in the demulsification of crude oil emulsions. Processes. 2019;7:470.

[6] Grenoble Z, Trabelsi S. Mechanisms, performance optimization and new developments in demulsification processes for oil and gas applications. Advances in Colloid and Interface Science. 2018;260:32–45.

[7] Kundu P, Mishra IM. Treatment and reclamation of hydrocarbon-bearing oily wastewater as a hazardous pollutant by different processes and technologies: a state-of-the-art review. Reviews in Chemical Engineering. 2018;35:73–108.

[8] Fang YY, Nie ZQ, Die QQ, Tian YJ, Liu F, He J, Huang QF. Spatial distribution, transport dynamics, and health risks of endosulfan at a contaminated site. Environmental Pollution. 2016;216:538–547.

[9] Wan WC, Lin YH, Prakash A, Zhou Y. Three-dimensional carbon-based architectures for oil remediation: From synthesis and modification to functionalization. Journal of Materials Chemistry A. 2016;4:18687–18705.

[10] Qiu LJ, Zhang RY, Zhang Y, Li CJ, Zhang Q, Zhou Y. Superhydrophobic, mechanically flexible and recyclable reduced graphene oxide wrapped sponge for highly efficient oil/water separation. Frontiers of Chemical Science and Engineering. 2018;12:390–399.

[11] Zolfaghari R, Fakhru'l-Razi A, Abdullah LC, Elnashaie SSEH, Pendashteh A. Demulsification techniques of water-in-oil and oil-in-water emulsions in petroleum industry. Separation and Purification Technology. 2016;170:377–407.

[12] Mohammadian E, Ariffin TST, Azdarpour A, Hamidi H, Yusof S, Sabet M, Yahya E. Demulsification of light malaysian crude oil emulsions using an electric field method. Industrial & Engineering Chemistry Research. 2018;57:13247–13256.

[13] Takahashi Y, Fukuyasu K, Horiuchi T, Kondo Y, Stroeve P. Photoinduced demulsification of emulsions using a photoresponsive gemini surfactant. Langmuir. 201;430:1-47.

[14] Zhang GF, Jiang JX, Zhang QH, Zhan XL, Chen FQ. Amphiphilic poly(ether sulfone) membranes for oil/water separation: Effect of sequence structure of the modifier. AICHE Journal. 2017;63:15365.

[15] Niu Z, Ma XM, Manica R, Yue T. Molecular destabilization mechanism of asphaltene model compound C_5Pe interfacial film by EO-PO copolymer: Experiments and MD simulation. Journal of Physical Chemistry C. 2019;123:10501–10508.

[16] Zaman H, Ali N, Shah AHA, Gao XY, Zhang SZ, Hong K, Bilal M. Effect of pH and salinity on stability and dynamic properties of magnetic composite amphiphilic demulsifier molecules at the oil-water interface. Journal of Molecular Liquids. 2019;290:111186.

[17] Shehzad F, Hussein IA, Kamal MS, Ahmad W, Sultan AS,Nasser MS. Polymeric surfactants and emerging alternatives used in the demulsification of produced water: A review. Polymer Reviews. 2018;58:63–101.

[18] Atta AM, Al-Lohedan HA, Abdullah MMS. Dipoles poly(ionic liquids) based on 2-acrylamido-2-methylpropane sulfonic acid-co-hydroxyethyl methacrylate for demulsification of crude oil water emulsions. Journal of Molecular Liquids. 2016;222:680–690.

[19] Guzman-Lucero D, Flores P, Rojo T, Martinez-Palou R. Ionic liquids as demulsifiers of water-in-crude oil emulsions: Study of the microwave effect. Energy & Fuels. 2010;24:3610–3615.

[20] Atta AM, Abdullah MMS, Al-Lohedan HA, Gaffer AK. Synthesis and application of amphiphilic poly(ionic liquid) dendron from cashew nut shell oil as a green oilfield chemical for heavy petroleum crude oil emulsion. Energy & Fuels. 2018;32:4873–4884.

[21] Lia ZW, Geng HK, Wang XJ, Jing B, Liu YF, Tan YB. Noval tannic acid-based polyether as an effective demulsifier for water-inaging crude oil emulsions. Chemical Engineering Journal. 2018;354:1110–1119.

[22] Huang XF, Liu WQ, Xiong YJ, Peng KM, Liu J, Lu LJ. Application and effect of functional magnetic nanoparticles in emulsion preparation and demulsification. Acta Physico-Chimica Sinica. 2018;34:49–64.

[23] Xu HY, Jia WH, Ren SR, Wang JP. Novel and recyclable demulsifiifier of expanded perlite grafted by magnetic nanoparticles for oil separation from emulsifiified oil wastewaters. Chemical Engineering Journal. 2018;337:10-18.

[24] Liu J, Wang HJ, Li XC, Jia WH, Zhao YP, Ren SL. Recyclable magnetic graphene oxide for rapid and effifficient demulsifiification of crude oil-in-water emulsion. Fuel. 2017;189:79-87.

[25] Song P, Natale G, Wang JY, Bond T, Hejazi H, Siegler HD, Gates I, Lu QY. 2D and 3D metal–organic framework at the oil/water interface: A Case Study of Copper Benzenedicarboxylate. Advanced Materials Interfaces. 2019;6:1801139.

[26] Vimont A, Goupil JM, Lavalley JC, Marco D, Suzy S, Christian S, Franck M, Gerard F, Nathalie A. Investigation of acid sites in a zeotypic giant pores chromium(III) carboxylate. Journal of the American Chemical Society. 2006;128:3218–3227.

[27] Jiang JC, Yaghi OM. Bronsted acidity in metal-organic frameworks. Chemical Reviews. 2015;115:6966–6997.

[28] Wang R, Xu HJ, Zhang K, Wei SY, Wu DY. High-quality Al@Fe-MOF prepared using Fe-MOF as a micro-reactor to improve adsorption performance for selenite. Journal of Hazardous Materials. 2019;364:272–280.

[29] Wang R, Xu HJ, Wei SY, Wu DY. The characteristice and mechanism of selenite adsorption by MOF-Fe. Acta Scientiae Circumstantiae. 2019;39:737–746.

[30] Temizel C, Canbaz CH, Tran H, Abdelfatah E, Jia B, Putra D, Irani M, Alkouh A. A Comprehensive review heavy oil reservoirs, latest techniques, discoveries, technologies and applications in the oil and gas industry. SPE International Heavy Oil Conference and Exhibition. 2018;193646-MS.

[31] Seo YK, Yoon JW, Lee JS, Lee UH, Hwang YK, Jun CH, Horcajada P, Serre C,Chang JS. Large scale fluorine-free synthesis of hierarchically porous iron(III) trimesate MIL-100(Fe) with a zeolite MTN topology. Microporous and Mesoporous Materials. 2012;157:137–145.

[32] Wang R. Formation, surface properties and selenite adsorption of MOF-Fe (In Chinese). Hubei Minzu University. 2019.

[33] Kerr YH, Waldteufel P, Wigneron JP, Delwart S, Cabot F, Boutin J, Escorihuela MJ, Font J,Reul N, Gruhier C, Juglea SE, Drinkwater MR, Hahne A, Martin-Neira M, Mecklenburg S. The SMOS mission: New tool for monitoring key elements of the global water cycle. Proceedings of the IEEE. 2010;98(5):666–687.

[34] Hazrati N, Beigi A.M, Abdouss M. Demulsification of water in crude oil emulsion using long chain imidazolium ionic liquids and optimization of parameters. Fuel. 2018;229:126–134.

[35] El-Sharaky EA, El-Tabey AE, Mishrif MR. Novel star polymeric nonionic surfactants as crude oil emulsion breakers. Journal of Surfactants and Detergents. 2019;22:779–793.

[36] Feitosa FX, Alves RS, de Sant'Ana HB. Synthesis and application of additives based on cardanol as demulsifier for water-in-oil emulsions. Fuel. 2019;245:21–28.

[37] Wang F, Fang SW, Duan M, Xiong Y, Wang XJ. Synthesis of a novel demulsifier by one-pot synthesis using two PEO-PPO demulsifiers as materials and the study of its demulsification performance. Separation Science and Technology. 2019;54:1233–1240.

[38] Liu J, Li XC, Jia WH, Ding MS, Zhang Y, Ren SL. Separation of emulsified oil from oily wastewater by functionalized multiwalled carbon nanotubes. Journal of Dispersion Science and Technology. 2016;37:1294–1302.

[39] Du YC, Si PC, Wei LQ, Wang YL, Te YB, Zuo GH, Yu B, Zhang XM, Ye SF. Demulsification of acidic oil-in-water emulsions driven by chitosan loaded $Ti_3C_2T_x$. Applied Surface Science. 2019;476:878–885.

[40] Sagdeev D, Gabitov I, Isyanov C, Khairutdinov V, Farakhov M, Zaripov Z, Abdulagatov I. Densities and viscosities of oleic acid at atomspheric pressure. Journal of the American Oil Chemists Society. 2019;96:647-662.

[41] Wang R, Gong Y, Xu HJ, Wei SY, Wu DY. Characteristics and adsorption properties of Se(IV) for MOF-Fe prepared with different conditioningagent (In Chinese). Chinese Journal of Inorganic Chemistry. 2018;34:906–916.